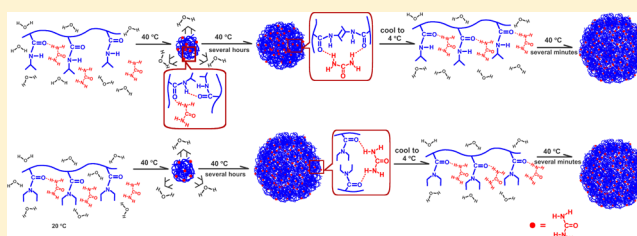


A Comparative Study of Urea-Induced Aggregation of Collapsed Poly(*N*-isopropylacrylamide) and Poly(*N,N*-diethylacrylamide) Chains in Aqueous Solutions

Yijie Lu,[†] Xiaodong Ye,^{*,†,‡} Kejin Zhou,^{§,||} and Wenjing Shi^{†,⊥}[†]Hefei National Laboratory for Physical Sciences at the Microscale, Department of Chemical Physics, and [‡]CAS Key Laboratory of Soft Matter Chemistry, University of Science and Technology of China, Hefei, Anhui 230026, China[§]Shanghai-Hong Kong Joint Laboratory in Chemical Synthesis, Shanghai Institute of Organic Chemistry, Chinese Academy of Science, 354 Fenglin Lu, Shanghai 200032, China

ABSTRACT: The urea-induced aggregation of poly(*N*-isopropylacrylamide) (PNIPAM) and poly(*N,N*-diethylacrylamide) (PDEAM) globules was studied by using a combination of static and dynamic light scattering. Our results have revealed that urea acting as a cross-linker via formation of two hydrogen bonds with the amide groups of PNIPAM and PDEAM in different globules causes the aggregation, and the aggregation of PNIPAM and PDEAM globules is a reaction-limited cluster–cluster aggregation (RLCA) process. The aggregates have a uniform sphere structure that may be due to the restructuring of the aggregates. The aggregation rate of PNIPAM globules is slower than that of PDEAM, which might mainly contribute to the reasons that the amide groups of PNIPAM have more chance to be inside the globules because of the formation of intra- and inter-hydrogen bonds and the smaller number density of the PNIPAM aggregates at the original time. When the aqueous urea solutions were cooled and reheated to 40 °C, the aggregation became faster than the first heating process, indicating that the urea molecules have replaced some water molecules binding to the amide groups at high temperature and some of the urea molecules remain interacting with the polymers even at the temperature lower than the cloud point temperature.



INTRODUCTION

Urea as a well-known protein denaturant has received much attention.^{1–5} Until now, two distinct mechanisms have been proposed to explain urea-induced denaturation behavior of proteins in aqueous solutions. One is that the direct interactions between proteins and urea, such as hydrogen bonds, electrostatic interactions, and van der Waals attractions, cause the denaturation of proteins.^{4–10} The other suggested that indirect interactions by changing water molecule structures and facilitating the hydration of nonpolar solutes are the reason for the denaturation.^{11–13} Recent studies including both theoretical simulations and spectroscopy studies showed that urea not only binds the charged and polar residues, but also significantly influences polar interactions within the protein backbone by binding carbonyl oxygen and includes the unfolding of secondary structures of proteins.^{9,14,15} Proteins contain different types of amino acids, which could form numerous secondary and tertiary structures. Thus, the analysis of the reason for the denaturation by spectroscopic methods, including both infrared and NMR spectroscopy, remains difficult because of the physiochemical complexity of proteins. For this reason, Cremer et al.¹⁶ used a thermally sensitive polymer poly(*N*-isopropylacrylamide) (PNIPAM) as a mimic for the cold denaturation of proteins and investigated whether there is direct hydrogen-bonding interactions between PNIPAM and urea. Their results from FTIR spectroscopy

and Stokes radius measurements clearly showed that through direct hydrogen bonding urea interacts with the amide groups in PNIPAM and stabilizes the aggregates of polymer. Note that PNIPAM undergoes a phase transition around 31 °C, and a collapsed globule of a single polymer chain or aggregates form depending on the concentration of polymers in aqueous solutions.^{17–20} During the phase transition, interchain and intrachain hydrogen bonds form.^{21–26} Another thermally sensitive polymer poly(*N,N*-diethylacrylamide) (PDEAM) with cloud point temperature (T_{cp}) around 30 °C could not form interchain or intrachain hydrogen bonds by themselves due to the absence of hydrogen donor site.^{27–31} The chemical structures of PNIPAM and PDEAM are shown in Figure 1.

The thermodynamic properties of these two model polymers have been extensively studied by laser light scattering,^{21,30} ultrasensitive differential scanning calorimetry,^{23,26,32,33} fluorescence spectroscopy,^{17,25} and Fourier transform infrared spectroscopy.^{22,24,29,31} The effect of urea on the conformational behavior of PNIPAM in dilute aqueous solutions was also investigated by fluorescence spectroscopy, including fluorescence quenching and fluorescence anisotropy measurements via pyrene probe and acenaphthylene label studies.³⁴ Besides,

Received: April 10, 2013

Revised: May 11, 2013

Published: May 15, 2013



Figure 1. Chemical structures of PDEAM and PNIPAM.

Zhang et al. investigated the effect of urea on the single-chain elasticity of PNIPAM and PDEAM by an atomic force microscopy-based single molecules force spectroscopy.^{35,36} However, little is known about whether globules of PNIPAM or PDEAM can be stable in aqueous urea solutions above LCST and what the aggregation behavior is if they are unstable. For this reason, in this Article, the aggregation behavior of the globules of PNIPAM and PDEAM in aqueous urea solutions has been studied by laser light scattering (LLS), as light scattering has been proven to be a particular useful method to study the kinetics of aggregation, and LLS is also a direct method to study the scaling relationship between the size and the molar mass of the aggregates. Our objective is to understand the effect of the intra/inter-hydrogen bonding on the stability of the globules of PNIPAM and PDEAM, and on the aggregation behavior in aqueous urea solutions as well.

We concluded neither PNIPAM nor PDEAM polymer chains could be stable in aqueous urea solutions when the concentration of urea was above a certain value at 40 °C. The aggregates of these polymer chains undergo a kinetic growth with time. The scaling analysis shows that these aggregates are uniform spheres instead of fractional aggregates. After the solution is cooled and reheated at the second heating process, the aggregation rate in urea solution was much faster than the first heating process, indicating that some urea molecules have replaced water molecules binding to the amide groups at high temperature and some of the urea molecules remain interacting with the polymers even at the temperature lower than the cloud point temperature.

MATERIALS

Details for the synthesis of the PNIPAM homopolymer can be found elsewhere.^{25,37} Briefly, monomer *N*-isopropylacrylamide was recrystallized three times in a benzene/*n*-hexane mixture. The purified monomer and recrystallized azobisisobutyronitrile (AIBN) as an initiator were dissolved in purified solvent benzene. The solution was degassed through three cycles of freezing and thawing, and the reaction was carried out at 56 °C for 30 h. The resultant PNIPAM homopolymer was carefully fractionated by the dissolution/precipitation process in a mixture of dry acetone and dry hexane at room temperature. *N,N*-Diethylacrylamide (DEAM) was prepared by reacting acryloyl chloride with an excess of diethylamine in methylene chloride at 0 °C.²⁷ The salt was removed by filtration, and solvent was evaporated. The product was purified by three-time vacuum distillation, yielding a clear liquid that was kept in a freezer before use. The purified monomer DEAM, with AIBN (0.2 mol % for monomer) as an initiator, was charged into a one-neck flask and then degassed by five cycles of freezing–pumping–thawing. The bulk polymerization was carried out at 25 °C for 30 days to yield a transparent solid. The resultant poly(*N,N*-diethylacrylamide) (PDEAM) was successively fractionated in a mixture of acetone and *n*-hexane (1:2).

Laser Light Scattering LLS. A commercial LLS spectrometer (ALV/DLS/SLS-5022F) equipped with a multi- τ digital time correlation (ALV5000) and a cylindrical 22-mW He–Ne laser ($\lambda_0 = 632$ nm, UNIPHASE) as the light source was used. In static LLS, we were able to obtain both apparent weight-average molar mass (M_w) and the z -averaged root-mean-square radius of gyration ($\langle R_g^2 \rangle_z^{1/2}$) (or written as $\langle R_g \rangle$) of polymer chains in a dilute solution from the angular dependence (15°–150°) of the excess absolute time-averaged scattered intensity, that is, the Rayleigh ratio $R_{v,v}(q)$ by eq 1:³⁸

$$\begin{aligned} \frac{KC}{R_{v,v}(q)} &\approx \frac{1}{M_w} \left(1 + \frac{1}{3} \langle R_g^2 \rangle_z q^2 \right) + 2A_2C \\ &\approx \frac{1}{M_w} \left(1 + \frac{1}{3} \langle R_g^2 \rangle_z q^2 \right) \end{aligned} \quad (1)$$

where $K = 4\pi^2 n^2 (dn/dC)^2 / (N_A \lambda_0^4)$ and $q = (4\pi n / \lambda_0) \sin(\theta/2)$ with n , λ_0 , θ , and A_2 being the solvent refractive index, the wavelength of light in vacuum, the scattering angle, and the second virial coefficient, respectively. In the present study, the polymer concentration is so low that the term of $2A_2C$ can be ignored.

In dynamic LLS,³⁹ the Laplace inversion of each measured intensity–intensity time correlation function $G^{(2)}(q,t)$ in the self-beating mode can lead to a line-width distribution $G(\Gamma)$, where q is the scattering vector. For dilute solutions, Γ is related to the translational diffusion coefficient D by $(\Gamma/q^2)_{C \rightarrow 0, q \rightarrow 0} \rightarrow D$, so that $G(\Gamma)$ can be converted into a translational diffusion coefficient distribution $G(D)$ or further a hydrodynamic radius distribution $f(R_h)$ via the Stokes–Einstein equation, $R_h = k_B T / 6\pi\eta_0 D$, where k_B , T , and η_0 are the Boltzmann constant, the absolute temperature, and the solvent viscosity, respectively.

The weight-average molar mass (M_w), the radius of gyration ($\langle R_g \rangle$), and the average hydrodynamic radius ($\langle R_h \rangle$) of polymer fractions used in our experiments were determined by a combination of static and dynamic light scattering, and the results are summarized in Table 1. The polydispersity index

Table 1. Laser Light Scattering Characterization of PNIPAM and PDEAM Samples Used at 20 °C

sample	M_w (g/mol)	M_w/M_n	$\langle R_g \rangle$ (nm)	$\langle R_h \rangle$ (nm)	$\langle R_g \rangle / \langle R_h \rangle$
PNIPAM	1.7×10^7	~1.2	205	139	1.47
PDEAM	1.7×10^7	~1.1	169	108	1.56

$(\langle M_w \rangle / \langle M_n \rangle)$ was estimated from the relative width $(\mu_2 / \langle \Gamma \rangle^2)$ of the line-width distribution ($G(\Gamma)$) measured in dynamic light scattering because $M_w/M_n \approx 1 + 4 \mu_2 / \langle \Gamma \rangle^2$. The urea solutions with a polymer concentration of 2×10^{-5} g/mL were placed in a LLS cell holder thermostatted at 40 °C. Time dependence of scattering light intensity and intensity–intensity time correlation function were measured during the aggregation. The average aggregation number $\langle N_{agg} \rangle$ was calculated from the ratio of the weight average molar masses of the aggregates to that of individual polymer chains measured by LLS.

RESULTS AND DISCUSSION

Individual PNIPAM and PDEAM chains in aqueous solutions were first characterized by a combination of static light scattering and dynamic light scattering. Table 1 summarized the values of $\langle M_w \rangle$, $\langle R_g \rangle$, and $\langle R_h \rangle$ of these two polymers in

water at 20 °C, where the concentration is 2×10^{-5} g/mL. From Table 1, we know that $\langle R_g \rangle$ and $\langle R_h \rangle$ of PDEAM are 169 and 108 nm, respectively. $\langle R_g \rangle$ and $\langle R_h \rangle$ of PNIPAM are 205 and 140 nm, respectively. Although these two polymers have the same weight-average molar mass as 1.7×10^7 g/mol, PNIPAM has a larger size than PDEAM, which may be due to more favorable interactions with water molecules and larger degree of polymerization as the repeating unit of PNIPAM has a smaller molar mass.^{30,37} The ratios of $\langle R_g \rangle / \langle R_h \rangle$ of both polymers ~ 1.5 are expected for linear flexible polymer chains in good solvent.

Figure 2 shows the time dependence of the average aggregation number $\langle N_{\text{agg}} \rangle$ of PDEAM and PNIPAM chains

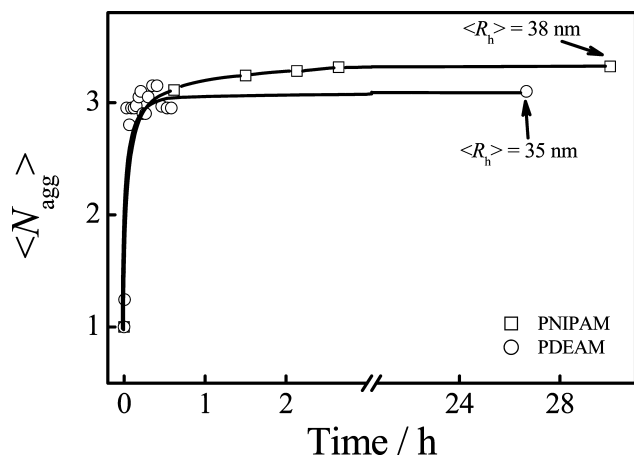


Figure 2. Time dependence of average aggregation number $\langle N_{\text{agg}} \rangle$ of PNIPAM and PDEAM when the temperature was jumped from 20 to 40 °C without addition of urea in water, where $C_{\text{PNIPAM}} = C_{\text{PDEAM}} = 2 \times 10^{-5}$ g/mL.

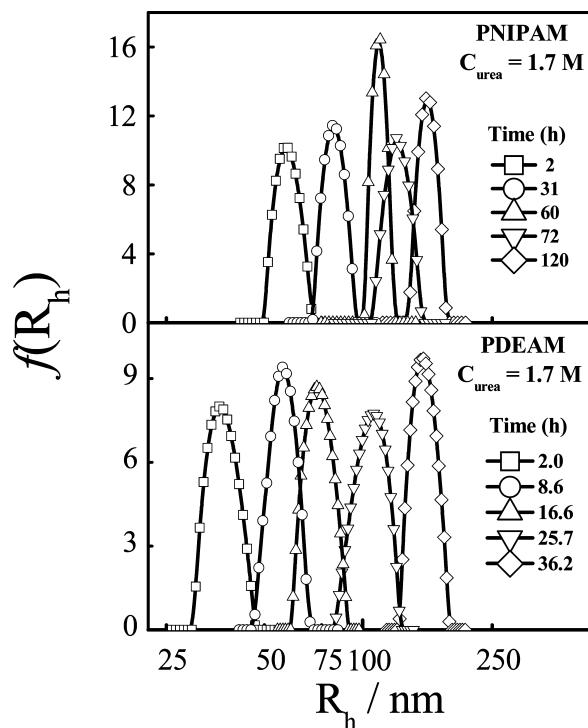


Figure 3. Time dependence of the hydrodynamic radius distribution $f(R_h)$ of PNIPAM and PDEAM aggregates in aqueous solutions at different time when the temperature was jumped from 20 to 40 °C, where $C_{\text{PNIPAM}} = C_{\text{PDEAM}} = 2 \times 10^{-5}$ g/mL, $C_{\text{urea}} = 1.7 \text{ M}$.

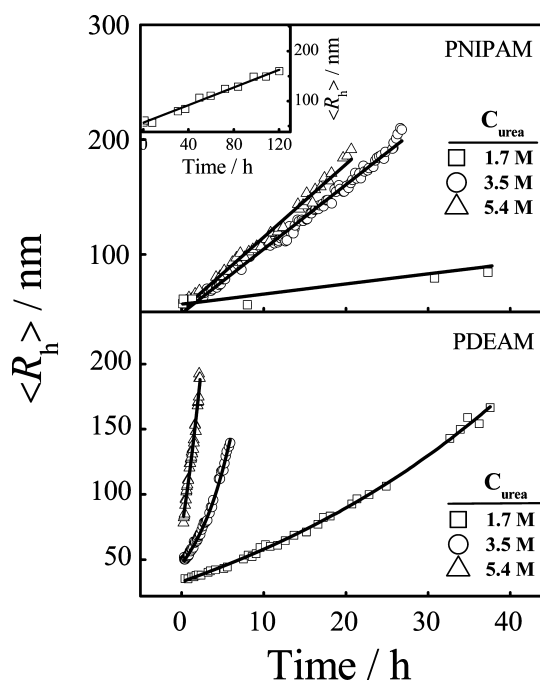


Figure 4. Time dependence of the average hydrodynamic radius $\langle R_h \rangle$ of PNIPAM and PDEAM aggregates in aqueous solutions with different concentrations of urea when the temperature was jumped from 20 to 40 °C, where $C_{\text{PNIPAM}} = C_{\text{PDEAM}} = 2 \times 10^{-5}$ g/mL. The $\langle R_h \rangle$ values of PNIPAM aggregates up to 40 h were also shown in the upper main plot of the upper layer.

in water without addition of urea when the temperature of the polymer solutions was jumped from 20 to 40 °C. Note that the average hydrodynamic radii of stable PNIPAM and PDEAM aggregates at 40 °C are 38 and 36 nm, respectively, which are much smaller than the $\langle R_h \rangle$ values of PNIPAM ($\langle R_h \rangle = 139$ nm) and PDEAM ($\langle R_h \rangle = 108$ nm) at 20 °C, as shown in Table 1. Meanwhile, the aggregates form within 1 h with $\langle N_{\text{agg}} \rangle \approx 3$ for both polymers and remain stable at least ~ 30 h. This could be attributed to the amphiphilic nature of NIPAM and DEAM monomers and a delicate balance between the hydrophobic backbone and hydrophilic motif, which stabilize the collapsed polymers in water as well as a negative charge carried by the mesoglobules mentioned by Winnik et al.²⁰

With the addition of urea, the globules of PNIPAM and PDEAM are unstable in aqueous solutions. From Laplace inversion, one can calculate the hydrodynamic radius distribution $f(R_h)$ by the CONTIN program provided by Provencher.^{40,41} Figure 3 shows the hydrodynamic radius distributions of the aggregates at different time when the temperature of the solutions was increased suddenly from 20 to 40 °C, where the concentration of urea is 1.7 M. From Figure 3, we know that the $\langle R_h \rangle$ increases with time and all of the aggregates have narrow size distributions at different time. Moreover, at the same time $t = 2$ h, $\langle R_h \rangle$ of PNIPAM aggregates is ~ 52 nm, which is larger than that of PDEAM aggregates.

Figure 4 shows the time dependence of the average hydrodynamic radius $\langle R_h \rangle$ of PNIPAM and PDEAM aggregates in aqueous solutions with different concentrations of urea when the temperature was jumped from 20 to 40 °C, where $C_{\text{PNIPAM}} = C_{\text{PDEAM}} = 2 \times 10^{-5}$ g/mL. For both polymers, the aggregation rate increases with the concentration of urea. When the concentration of urea was less than 1.7 M, we did not observe

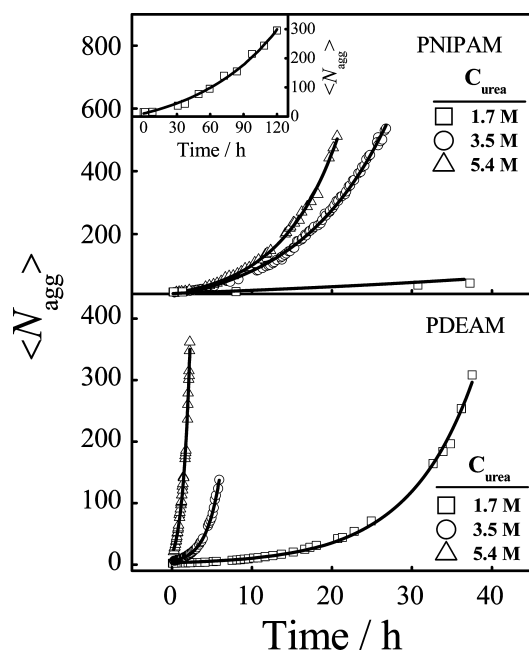


Figure 5. Time dependence of average aggregation number $\langle N_{agg} \rangle$ of PNIPAM and PDEAM aggregates in aqueous solutions with different concentrations of urea when the temperature was jumped from 20 to 40 °C, where $C_{PNIPAM} = C_{PDEAM} = 2 \times 10^{-5}$ g/mL. The $\langle N_{agg} \rangle$ values of PNIPAM aggregates up to 40 h were also shown in the main plot of the upper layer.

obvious aggregation in 1 day. Besides, with the same concentration of urea, PDEAM aggregates faster than PNIPAM. By Fourier transform infrared spectroscopy (FTIR) and Stokes radius measurements, Cremer et al. reported that the decrease in the lower critical solution temperature (LCST) with the addition of urea was due to the direct hydrogen bonding of urea to the amide groups of PNIPAM.¹⁶ The two NH_2 groups of urea can form hydrogen bonds with amide groups, indicating that urea can act as a cross-linker in the aggregation via the formation of two hydrogen bonds. Furthermore, the amide groups of PNIPAM and PDEAM, which are more hydrophilic groups as compared to the hydrophobic backbone, may localize at the surface of the globules, which facilitates the formation of the hydrogen bonds with urea at higher temperature. Cremer et al. also showed that when the concentration of urea is less than ~ 1 M, the fraction of urea bound to PNIPAM is as small as ~ 0.02 in H_2O and ~ 0 in D_2O .¹⁶ This may be the reason that there is no aggregation when the concentration of urea is less than 1.7 M. For PDEAM, the aggregation process follows an exponential kinetics, that is, $R \approx e^{At}$, where A is a constant, indicating a reaction-limited cluster–cluster aggregation (RLCA). The A values are 0.024, 0.20, and 0.21 h^{-1} for the solutions with the concentration of urea as 1.7, 3.5, and 5.4 M, respectively. For PNIPAM, the average hydrodynamic radius $\langle R_h \rangle$ increases linearly with time,

which may be due to the fact that the aggregation process is an initial stage in a RLCA as $\langle R_h \rangle \propto e^{At} \propto At$ when At is smaller than 1. Because $\langle R_h \rangle$ is a complicate parameter, which involves both the structure and the hydrodynamic draining, in this experiment we use average aggregation number $\langle N_{agg} \rangle$ to analyze the aggregation kinetics.

Figure 5 shows the average aggregation number $\langle N_{agg} \rangle$ increased exponentially with time for both PNIPAM and PDEAM at different concentrations of urea, further indicating that the aggregation is a RLCA process. The aggregation rate of PNIPAM is slower than that of PDEAM with the same concentration of urea. The results of the fitting are shown in Figure 5, and the fitting parameters are tabulated in Table 2, where k represents the apparent first-order rate coefficient during the aggregation. Note that at $t = 0$, the aggregation number $\langle N_{agg} \rangle_{t=0}$ equals $A + y_0$, as shown in Table 2. The $\langle N_{agg} \rangle_{t=0}$ values at different concentrations of urea are not smaller than 1, indicating the formation of aggregates at $t = 0$. Because of the relatively large errors of $\langle N_{agg} \rangle_{t=0}$ values, we did not study the effect of the urea concentration on $\langle N_{agg} \rangle_{t=0}$. We examine the urea concentration dependence of k in more detail in Figure 6. Because the size of PNIPAM aggregates is larger than that of the PDEAM aggregates at the beginning of the aggregation, the number density of the PNIPAM aggregates is smaller than that of PDEAM aggregates as both of the concentrations are 2×10^{-5} g/mL. Thus, the aggregation rate coefficient of PNIPAM is smaller. Another possible reason for the lower aggregation rate of PNIPAM than that of PDEAM is that PNIPAM can form intra- or interchain hydrogen bonds, whereas PDEAM cannot. During the formation of small aggregates when the temperature was increased from 20 to 40 °C, the NH group in the amide group of PNIPAM whose carbonyl group has formed a hydrogen bond with urea may form intra- and/or interchain hydrogen bonds with the carbonyl group of another repeating unit in the same or different polymer chains. That is to say, the amide groups of PNIPAM have more chance to be inside the globules, and the number of urea molecules that form hydrogen bonds with the amide groups of PNIPAM on the surface of the aggregates is smaller. As we mentioned before, it has been reported that the fraction of urea bound to PNIPAM is negligible when the concentration of urea (C_{urea}) is below a certain value of ~ 1 M, and the fraction increases linearly with the C_{urea} when C_{urea} is above this value.¹⁶ For this reason, it is expected that no aggregation can be observed by laser light scattering when the concentration is below a critical urea concentration ~ 1.2 M for both PNIPAM and PDEAM because there is almost no urea bound to the surface of the globule, as shown in Figure 6. The existence of a critical urea concentration ($C_{urea,c}$) for the aggregation in our study may be compared to the results from the denaturation of proteins by urea using fluorescence techniques, circular dichroism, and other methods. These experiments showed that the fraction of unfolded protein is constant at 0 when the urea concentration is lower than a

Table 2. Aggregation Kinetics of PNIPAM and PDEAM in Aqueous Urea Solutions with Different Concentrations at 40 °C Analyzed by the Exponential Function $\langle N_{agg} \rangle = A \cdot \exp(kt) + y_0$

C_{urea} (M)	PNIPAM				PDEAM			
	A	k (h^{-1})	y_0	$\langle N_{agg} \rangle_{t=0} = A + y_0$	A	k (h^{-1})	y_0	$\langle N_{agg} \rangle_{t=0} = A + y_0$
1.7	72 ± 16	0.014 ± 0.002	-62 ± 18	10 ± 34	3.2 ± 0.4	0.121 ± 0.004	-0.3 ± 1.3	3 ± 2
3.5	49 ± 2	0.088 ± 0.002	-48 ± 4	1 ± 6	4.3 ± 0.3	0.59 ± 0.01	1.2 ± 0.7	6 ± 1
5.4	20 ± 2	0.138 ± 0.004	-13 ± 3	7 ± 5	34 ± 4	1.06 ± 0.04	-19 ± 6	15 ± 10

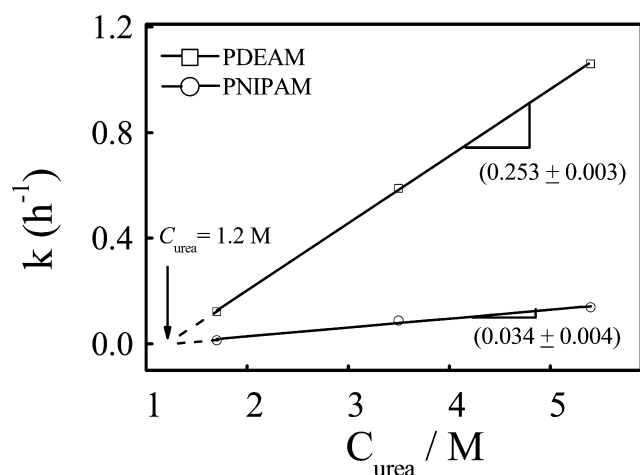


Figure 6. Urea concentration dependence of the PNIPAM/PDEAM aggregation kinetics.

Table 3. Critical Concentration of Urea ($C_{\text{urea},c}$) As Determined by Different Methods

proteins	$C_{\text{urea},c}$ (M)	methods	ref
apomyoglobin	1.6	fluorescence	43
ervatamin A	1.1	fluorescence	44
procerain	1.1 (pH = 2) 2.0 (pH = 3)	far-UV CD	45
β 1, a mutant form of the protein G B1 domain	2.7	size exclusion chromatography	46
AcK120 DBD	2.6	fluorescence	47

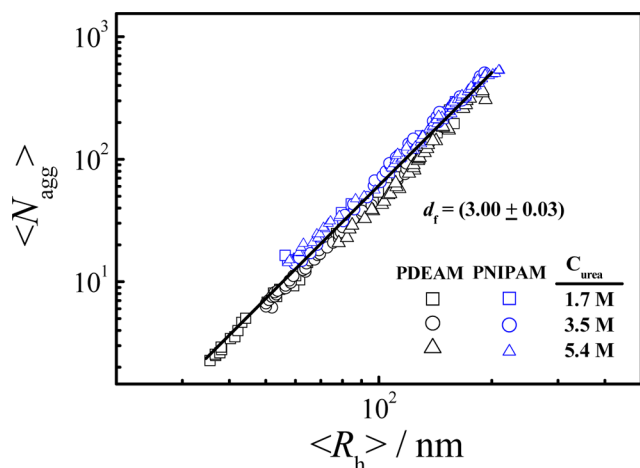


Figure 7. Double logarithmic plots of the average aggregation number $\langle N_{\text{agg}} \rangle$ of the aggregates versus the hydrodynamic radius $\langle R_h \rangle$ of PNIPAM and PDEAM aggregates in aqueous solutions with different urea concentrations, where $C_{\text{PNIPAM}} = C_{\text{PDEAM}} = 2 \times 10^{-5}$ g/mL.

critical concentration and increases with increasing urea concentration above this concentration. $C_{\text{urea},c}$ values for different proteins have been summarized in Table 3. From Table 3, we can see that even though these proteins are different, the $C_{\text{urea},c}$ is in the range of 1.1–2.7 M, indicating that urea might form hydrogen bonds with the amide groups on the first shell of proteins when the concentration is higher than $C_{\text{urea},c}$ like the situation in the current study.⁴²

Figure 7 shows double logarithmic plots of the average aggregation number $\langle N_{\text{agg}} \rangle$ of the aggregates versus the hydrodynamic radius $\langle R_h \rangle$ of PNIPAM and PDEAM in

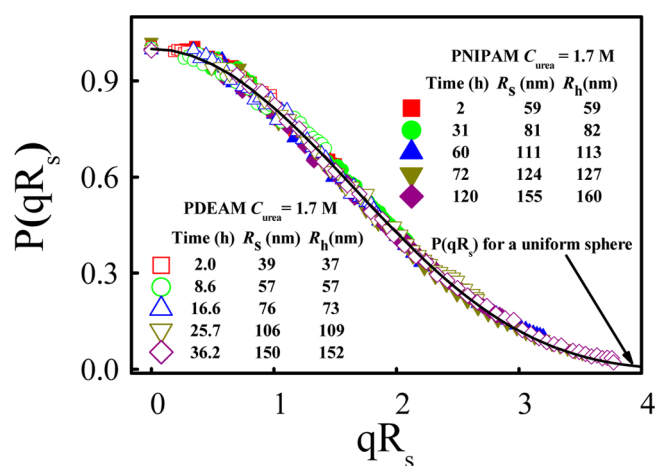


Figure 8. qR_s -dependence of scattering factor $P(qR_s)$ of PNIPAM and PDEAM aggregates formed at different time. The dark line is the scattering factor of a uniform sphere.

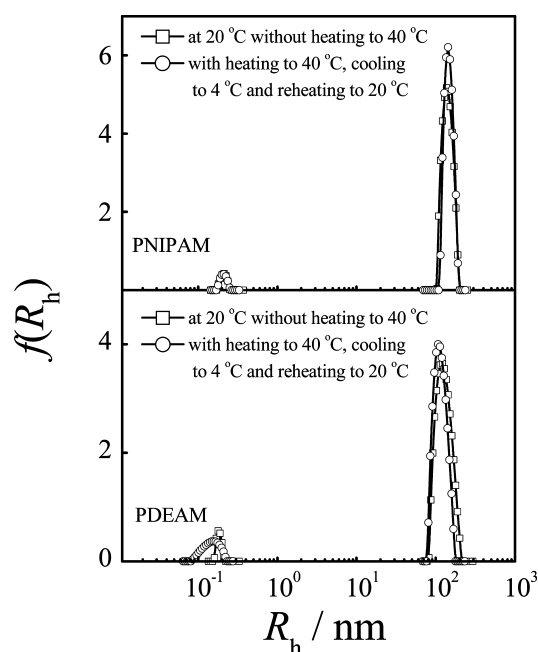


Figure 9. The hydrodynamic radius distribution $f(R_h)$ of the PNIPAM and PDEAM solution at 20 °C before and after heating to 40 °C, where $C_{\text{PNIPAM}} = C_{\text{PDEAM}} = 2 \times 10^{-5}$ g/mL, $C_{\text{urea}} = 3.5$ M.

aqueous solutions with different urea concentrations. We see that all data collapse into a single line of $\langle N_{\text{agg}} \rangle \propto \langle R_h \rangle^{d_f}$ with the dimension $d_f = (3.00 \pm 0.03)$, which means that the concentration of urea only influences the aggregation rates and the sizes but does not affect the aggregate structure. The d_f is ~ 3 in our study, which indicates the aggregates have a uniform density.

To further confirm the aggregates of these two polymers have a spherical structure, the scattering factors $P(qR_s)$ were obtained by static light scattering, and qR_s -dependence of scattering factor $P(qR_s)$ of PNIPAM and PDEAM aggregates formed at different time is shown in Figure 8. Theoretically, for a sphere the scattering factor is $P(qR_s) = [3(qR_s)^{-3}(\sin(qR_s) - qR_s \cos(qR_s))]^2$, where R_s and q are the radius of the sphere and the scattering vector, respectively. Figure 8 clearly shows that the experimental data are well represented by $P(qR_s)$ for a

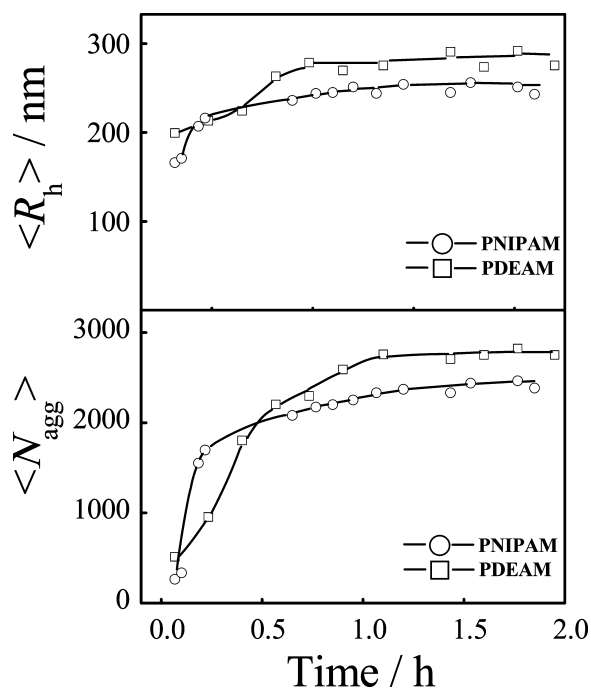


Figure 10. Time dependence of the average hydrodynamic radius $\langle R_h \rangle$ and the average aggregation number $\langle N_{agg} \rangle$ during the second heating process, where $C_{PNIPAM} = C_{PDEAM} = 2 \times 10^{-5}$ g/mL.

uniform sphere for both PNIPAM aggregates and PDEAM aggregates at different time, which means that these aggregates have a sphere structure rather than a fractal structure formed by diffusion limited cluster–cluster aggregation (DLCA) with a fractal dimension $d_f \approx 1.75$ – 1.80 or RLCA with a higher d_f in the range ~ 2.0 – 2.5 .⁴⁸ The results from Figure 4 and 5 indicate that the aggregation of PNIPAM and PDEAM is a RLCA process. Whereas Figure 8 shows the aggregates are uniform spheres, implying that the hydrogen-bonding interactions between PNIPAM and PDEAM globules are not very strong, so the globules can rearrange themselves in the aggregates to form uniform spheres with a large dimension of 3. Assuming that restructuring can happen immediately after two clusters have contacted each other, Meakin and Jullien found the fractal dimension increases from 1.80 to ~ 2.2 for DLCA and the increase in d_f is smaller for RLCA.⁴⁹ It should be noted that in their models, no subsequent restructuring is allowed, which may happen in the real system like ours and further increases

the d_f to 3. Note that for a sphere, the radius of sphere is the same as the hydrodynamics radius R_h of the sphere.⁵⁰ We can see that in our experiments the average hydrodynamic radius ($\langle R_h \rangle$) of these aggregates obtained from Figure 3 is very close to R_s values fitted in Figure 8.

Irreversible folding transitions of proteins induced by denaturants like guanidine hydrochloride or urea have been reported, which shows a hysteresis under folding/unfolding process.^{51–53} To check the reversibility of the aggregation process of PNIPAM or PDEAM in urea solutions, we cooled the solution of aggregates to 4 °C overnight. First, the two aqueous solutions were characterized by dynamic light scattering again at 20 °C. Figure 9 shows that there is little difference between the hydrodynamic radius distribution before and after the heating process where the concentration of urea is 3.5 M, indicating that the polymer aggregates could dissociate and return to its coil state. The small peak at ~ 0.2 nm was attributed to urea molecules in water because the size is similar to that of urea molecules.⁵⁴ When the solutions were increased from 20 to 40 °C again, the aggregation kinetics was much more different from that as shown in Figures 3 and 4. This time, large aggregates formed in a very short time, as shown in Figure 10. The faster aggregation rate indicates that urea molecules have replaced some water molecules binding to the amide groups at high temperature and some of the urea molecules remain interacting with the polymers even at the temperature lower than the cloud point temperature. Because of the small size of the binding urea, we cannot observe the change of the hydrodynamic radius of the polymer from Figure 9. However, this behavior is very similar to the hysteresis phenomena of PNIPAM chains in water, which is due to the incomplete removal of the interchain hydrogen bonds formed in the collapsed state during the dehydration.²⁴ Another possible additional reason attributed to the difference is that after the chain collapse at higher temperatures, most of the hydrophilic amide groups will be forced to stay outside. Thus, in the reheating process, these amide groups might be more available to induce the interchain association. Figure 11 shows the schematic diagram of the urea-induced aggregation during the first and second heating processes.

CONCLUSION

The aggregation kinetics of PNIPAM and PDEAM globules in urea aqueous solutions has been studied by laser light scattering. Our results show that the aggregation of PNIPAM

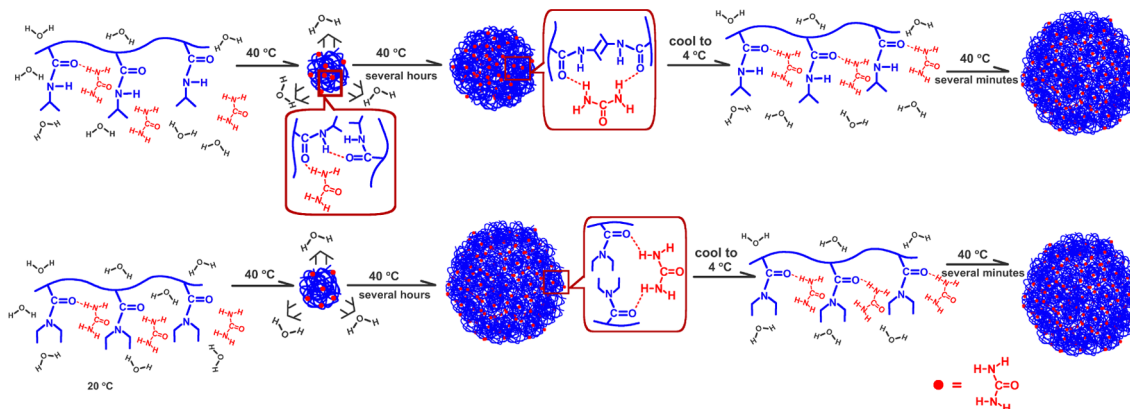


Figure 11. Schematic diagram of urea-induced aggregation of PNIPAM (upper row) and PDEAM (lower row) globules at 40 °C during the first and second heating processes.

and PDEAM polymer chains is a RLCA process. The aggregation rate of PDEAM is much faster than that of PNIPAM, which may be due to the smaller number density of the PNIPAM aggregates at the original time and the lower number density of amide groups on the surface of PNIPAM globules because of the possible formation of intra- and/or inter-hydrogen bonds. The aggregates of PNIPAM and PDEAM have a uniform sphere structure. After the solutions were cooled and reheated at the second heating process, the aggregates grow much faster, which indicates that the urea molecules have replaced some water molecules binding to the amide groups at high temperature and some of the urea molecules remain interacting with the polymers even at the temperature lower than the cloud point temperature.

AUTHOR INFORMATION

Corresponding Author

*Phone: 86-551-63606742. E-mail: xdye@ustc.edu.cn.

Present Addresses

^{||}Department of Pharmacology, Simmons Comprehensive Cancer Center, UT, Southwestern Medical Center at Dallas, 5323 Harry Hines Boulevard, Dallas, Texas 75390, United States.

[⊥]Department of Chemistry, The Chinese University of Hong Kong, Shatin, N. T., Hong Kong.

Notes

The authors declare no competing financial interest.

ACKNOWLEDGMENTS

We thank Prof. Chi Wu and Prof. Guangzhao Zhang for their valuable comments about the manuscript. We also thank reviewers for their useful comments. The financial support of the National Natural Scientific Foundation of China (NNSFC) Projects (21274140), the National Program on Key Basic Research Project (2012CB933802), and the Scientific Research Foundation for the Returned Overseas Chinese Scholars, State Education Ministry, is gratefully acknowledged.

REFERENCES

- (1) Kauzmann, W. Some Factors in the Interpretation of Protein Denaturation. *Adv. Protein Chem.* **1959**, *14*, 1–63.
- (2) Pace, C. N. Determination and Analysis of Urea and Guanidine Hydrochloride Denaturation Curves. *Methods Enzymol.* **1986**, *131*, 266–280.
- (3) Kresheck, G. C. Aqueous Solutions of Amphiphiles and Macromolecules. In *Water-A Comprehensive Treatise*; Franks, F., Ed.; Plenum Press: New York, 1975; Vol. 4.
- (4) Klimov, D. K.; Straub, J. E.; Thirumalai, D. Aqueous Urea Solution Destabilizes a Beta(16–22) Oligomers. *Proc. Natl. Acad. Sci. U.S.A.* **2004**, *101*, 14760–14765.
- (5) Hua, L.; Zhou, R. H.; Thirumalai, D.; Berne, B. J. Urea Denaturation by Stronger Dispersion Interactions with Proteins Than Water Implies a 2-Stage Unfolding. *Proc. Natl. Acad. Sci. U.S.A.* **2008**, *105*, 16928–16933.
- (6) Robinson, D. R.; Jencks, W. P. Effect of Compounds of Urea-Guanidinium Class on Activity Coefficient of Acetyltetraglycine Ethyl Ester and Related Compounds. *J. Am. Chem. Soc.* **1965**, *87*, 2462–2470.
- (7) Wallqvist, A.; Covell, D. G.; Thirumalai, D. Hydrophobic Interactions in Aqueous Urea Solutions with Implications for the Mechanism of Protein Denaturation. *J. Am. Chem. Soc.* **1998**, *120*, 427–428.

(8) Auton, M.; Holthauzen, L. M. F.; Bolen, D. W. Anatomy of Energetic Changes Accompanying Urea-Induced Protein Denaturation. *Proc. Natl. Acad. Sci. U.S.A.* **2007**, *104*, 15317–15322.

(9) O'Brien, E. P.; Dima, R. I.; Brooks, B.; Thirumalai, D. Interactions between Hydrophobic and Ionic Solutes in Aqueous Guanidinium Chloride and Urea Solutions: Lessons for Protein Denaturation Mechanism. *J. Am. Chem. Soc.* **2007**, *129*, 7346–7353.

(10) Stumpe, M. C.; Grubmuller, H. Interaction of Urea with Amino Acids: Implications for Urea-Induced Protein Denaturation. *J. Am. Chem. Soc.* **2007**, *129*, 16126–16131.

(11) Wetlaufer, D. B.; Coffin, R. L.; Malik, S. K.; Stoller, L. Nonpolar Group Participation in Denaturation of Proteins by Urea + Guanidinium Salts. Model Compound Studies. *J. Am. Chem. Soc.* **1964**, *86*, 508–514.

(12) Pace, N. C.; Tanford, C. Thermodynamics of Unfolding of β -Lactoglobulin A in Aqueous Urea Solutions between 5 and 55 Degrees. *Biochemistry* **1968**, *7*, 198–208.

(13) Frank, H. S.; Franks, F. Structural Approach to Solvent Power of Water for Hydrocarbons - Urea as a Structure Breaker. *J. Chem. Phys.* **1968**, *48*, 4746–4757.

(14) Das, A.; Mukhopadhyay, C. Urea-Mediated Protein Denaturation: A Consensus View. *J. Phys. Chem. B* **2009**, *113*, 12816–12824.

(15) Lim, W. K.; Rosgen, J.; Englander, S. W. Urea, but Not Guanidinium, Destabilizes Proteins by Forming Hydrogen Bonds to the Peptide Group. *Proc. Natl. Acad. Sci. U.S.A.* **2009**, *106*, 2595–2600.

(16) Sagle, L. B.; Zhang, Y. J.; Litosh, V. A.; Chen, X.; Cho, Y.; Cremer, P. S. Investigating the Hydrogen-Bonding Model of Urea Denaturation. *J. Am. Chem. Soc.* **2009**, *131*, 9304–9310.

(17) Winnik, F. M. Fluorescence Studies of Aqueous-Solutions of Poly(*N*-isopropylacrylamide) Below and above Their LCST. *Macromolecules* **1990**, *23*, 233–242.

(18) Wu, C.; Zhou, S. Q. Thermodynamically Stable Globule State of a Single Poly(*N*-isopropylacrylamide) Chain in Water. *Macromolecules* **1995**, *28*, 5388–5390.

(19) Wu, C.; Zhou, S. Q. First Observation of the Molten Globule State of a Single Homopolymer Chain. *Phys. Rev. Lett.* **1996**, *77*, 3053–3055.

(20) Kujawa, P.; Aseyev, V.; Tenhu, H.; Winnik, F. M. Temperature-Sensitive Properties of Poly(*N*-isopropylacrylamide) Mesoglobules Formed in Dilute Aqueous Solutions Heated above Their Demixing Point. *Macromolecules* **2006**, *39*, 7686–7693.

(21) Wang, X. H.; Qiu, X. P.; Wu, C. Comparison of the Coil-to-Globule and the Globule-to-Coil Transitions of a Single Poly(*N*-isopropylacrylamide) Homopolymer Chain in Water. *Macromolecules* **1998**, *31*, 2972–2976.

(22) Maeda, Y.; Nakamura, T.; Ikeda, I. Changes in the Hydration States of Poly(*N*-alkylacrylamide)s During Their Phase Transitions in Water Observed by FTIR Spectroscopy. *Macromolecules* **2001**, *34*, 1391–1399.

(23) Ding, Y. W.; Ye, X. D.; Zhang, G. Z. Microcalorimetric Investigation on Aggregation and Dissolution of Poly(*N*-isopropylacrylamide) Chains in Water. *Macromolecules* **2005**, *38*, 904–908.

(24) Cheng, H.; Shen, L.; Wu, C. LLS and FTIR Studies on the Hysteresis in Association and Dissociation of Poly(*N*-isopropylacrylamide) Chains in Water. *Macromolecules* **2006**, *39*, 2325–2329.

(25) Ye, X. D.; Lu, Y. J.; Shen, L.; Ding, Y. W.; Liu, S. L.; Zhang, G. Z.; Wu, C. How Many Stages in the Coil-to-Globule Transition of Linear Homopolymer Chains in a Dilute Solution? *Macromolecules* **2007**, *40*, 4750–4752.

(26) Ding, Y. W.; Ye, X. D.; Zhang, G. Z. Can Coil-to-Globule Transition of a Single Chain Be Treated as a Phase Transition? *J. Phys. Chem. B* **2008**, *112*, 8496–8498.

(27) Idziak, I.; Avoce, D.; Lessard, D.; Gravel, D.; Zhu, X. X. Thermosensitivity of Aqueous Solutions of Poly(*N,N*-diethylacrylamide). *Macromolecules* **1999**, *32*, 1260–1263.

(28) Lessard, D. G.; Ousalem, M.; Zhu, X. X. Effect of the Molecular Weight on the Lower Critical Solution Temperature of Poly(*N,N*-diethylacrylamide) in Aqueous Solutions. *Can. J. Chem.* **2001**, *79*, 1870–1874.

- (29) Maeda, Y.; Nakamura, T.; Ikeda, I. Change in Solvation of Poly(*N,N*-Diethylacrylamide) During Phase Transition in Aqueous Solutions as Observed by IR Spectroscopy. *Macromolecules* **2002**, *35*, 10172–10177.
- (30) Zhou, K. J.; Lu, Y. J.; Li, J. F.; Shen, L.; Zhang, G. Z.; Xie, Z. W.; Wu, C. The Coil-to-Globule-to-Coil Transition of Linear Polymer Chains in Dilute Aqueous Solutions: Effect of Intrachain Hydrogen Bonding. *Macromolecules* **2008**, *41*, 8927–8931.
- (31) Lu, Y. J.; Zhou, K. J.; Ding, Y. W.; Zhang, G. Z.; Wu, C. Origin of Hysteresis Observed in Association and Dissociation of Polymer Chains in Water. *Phys. Chem. Chem. Phys.* **2010**, *12*, 3188–3194.
- (32) Liu, H. Y.; Zhu, X. X. Lower Critical Solution Temperatures of *N*-Substituted Acrylamide Copolymers in Aqueous Solutions. *Polymer* **1999**, *40*, 6985–6990.
- (33) Ye, X. D.; Ding, Y. W.; Li, J. F. Scaling of the Molecular Weight-Dependent Thermal Volume Transition of Poly(*N*-isopropylacrylamide). *J. Polym. Sci., Part B: Polym. Phys.* **2010**, *48*, 1388–1393.
- (34) Fang, Y.; Qiang, J. C.; Hu, D. D.; Wang, M. Z.; Cui, Y. L. Effect of Urea on the Conformational Behavior of Poly(*N*-isopropylacrylamide). *Colloid Polym. Sci.* **2001**, *279*, 14–21.
- (35) Zhang, W. K.; Zou, S.; Wang, C.; Zhang, X. Single Polymer Chain Elongation of Poly(*N*-isopropylacrylamide) and Poly(acrylamide) by Atomic Force Microscopy. *J. Phys. Chem. B* **2000**, *104*, 10258–10264.
- (36) Wang, C.; Shi, W. Q.; Zhang, W. K.; Zhang, X.; Katsumoto, Y.; Ozaki, Y. Force Spectroscopy Study on Poly(acrylamide) Derivatives: Effects of Substitutes and Buffers on Single-Chain Elasticity. *Nano Lett.* **2002**, *2*, 1169–1172.
- (37) Zhou, S. Q.; Fan, S. Y.; Auyeung, S. C. F.; Wu, C. Light-Scattering-Studies of Poly(*N*-isopropylacrylamide) in Tetrahydrofuran and Aqueous-Solution. *Polymer* **1995**, *36*, 1341–1346.
- (38) Zimm, B. H. Apparatus and Methods for Measurement and Interpretation of the Angular Variation of Light Scattering - Preliminary Results on Polystyrene Solutions. *J. Chem. Phys.* **1948**, *16*, 1099–1116.
- (39) Chu, B. *Laser Light Scattering*, 2nd ed.; Academic Press: New York, 1991.
- (40) Provencher, S. W. Contin - a General-Purpose Constrained Regularization Program for Inverting Noisy Linear Algebraic and Integral-Equations. *Comput. Phys. Commun.* **1982**, *27*, 229–242.
- (41) Provencher, S. W. A Constrained Regularization Method for Inverting Data Represented by Linear Algebraic or Integral-Equations. *Comput. Phys. Commun.* **1982**, *27*, 213–227.
- (42) TiradoRives, J.; Orozco, M.; Jorgensen, W. L. Molecular Dynamics Simulations of the Unfolding of Barnase in Water and 8 M Aqueous Urea. *Biochemistry* **1997**, *36*, 7313–7329.
- (43) Deyoung, L. R.; Dill, K. A.; Fink, A. L. Aggregation and Denaturation of Apomyoglobin in Aqueous Urea Solutions. *Biochemistry* **1993**, *32*, 3877–3886.
- (44) Nallamsetty, S.; Dubey, V. K.; Pande, M.; Ambasht, P. K.; Jagannadham, M. V. Accumulation of Partly Folded States in the Equilibrium Unfolding of Ervatamin A: Spectroscopic Description of the Native, Intermediate, and Unfolded States. *Biochimie* **2007**, *89*, 1416–1424.
- (45) Dubey, V. K.; Jagannadham, M. V. Differences in the Unfolding of Procerain Induced by Ph, Guanidine Hydrochloride, Urea, and Temperature. *Biochemistry* **2003**, *42*, 12287–12297.
- (46) Ferreon, A. C. M.; Bolen, D. W. Thermodynamics of Denaturant-Induced Unfolding of a Protein That Exhibits Variable Two-State Denaturation. *Biochemistry* **2004**, *43*, 13357–13369.
- (47) Arbely, E.; Natan, E.; Brandt, T.; Allen, M. D.; Veprintsev, D. B.; Robinson, C. V.; Chin, J. W.; Joerger, A. C.; Fersht, A. R. Acetylation of Lysine 120 of PS3 Endows DNA-Binding Specificity at Effective Physiological Salt Concentration. *Proc. Natl. Acad. Sci. U.S.A.* **2011**, *108*, 8251–8256.
- (48) Weitz, D. A.; Huang, J. S.; Lin, M. Y.; Sung, J. Limits of the Fractal Dimension for Irreversible Kinetic Aggregation of Gold Colloids. *Phys. Rev. Lett.* **1985**, *54*, 1416–1419.
- (49) Meakin, P.; Jullien, R. The Effects of Restructuring on the Geometry of Clusters Formed by Diffusion-Limited, Ballistic, and Reaction-Limited Cluster Cluster Aggregation. *J. Chem. Phys.* **1988**, *89*, 246–250.
- (50) Teraoka, I. *Polymer Solutions: An Introduction to Physical Properties*; John Wiley & Sons, Inc.: New York, 2002.
- (51) Fuchs, A.; Seiderer, C.; Seckler, R. In Vitro Folding Pathway of Phage P22 Tailspike Protein. *Biochemistry* **1991**, *30*, 6598–6604.
- (52) Lai, Z. H.; McCulloch, J.; Lashuel, H. A.; Kelly, J. W. Guanidine Hydrochloride-Induced Denaturation and Refolding of Transthyretin Exhibits a Marked Hysteresis: Equilibria with High Kinetic Barriers. *Biochemistry* **1997**, *36*, 10230–10239.
- (53) Schuler, B.; Rachel, R.; Seckler, R. Formation of Fibrous Aggregates from a Non-Native Intermediate: The Isolated P22 Tailspike Beta-Helix Domain. *J. Biol. Chem.* **1999**, *274*, 18589–18596.
- (54) Jin, F.; Ye, J.; Hong, L.; Lam, H.; Wu, C. Slow Relaxation Mode in Mixtures of Water and Organic Molecules: Supramolecular Structures or Nanobubbles? *J. Phys. Chem. B* **2007**, *111*, 2255–2261.